MATEC Web of Conferences **77**, 08003 (2016) DOI: 10.1051/matecconf/20167708003
ICMMR 2016

Performance analysis of the plastic square plate based on the fiber reinforced PA66

Jian Wang , Junhong Zhang, Weidong Li, Zhexuan Xu

State Key Laboratory of Engines, Tianjin University, Tianjin 300072, People's Republic of China

Abstract. As the plastic component has the advantage of the lightweight, they are used widely in the industry and many researches are conducted simultaneously; In this study, combined the elastic constitutive model and the fiber orientation, the simulations of the plastic square plate with two material definitions are carried out. They are the orthotropic material and the anisotropic material respectively. Through the simulation comparisons, the anisotropic behaviors on the thermal field, the pressure field and the vibration characteristics of the fiber reinforced PA66 are all analyzed. The results show that the different material definitions have important influence on the structure analysis. It offers the guidance for the design and analysis of the plastic component.

1 Introduction

In recent years, the plastic components are applied in the mechanical industry widely, especially the automobile industry. The plastic components include the intake manifold, the oil cooler cover, the gear cover, the oil pan and so on. The engineering plastic has the advantage of the low density, high damping ratio, strong corrosion resistance, and good manufacture ability [1-3]. Therefore, the plastic component has the benefits of the lightweight, high strength, low noise and high productivity. As the density of the plastic is small and the price is equal to the metal, the cost price of the plastic component is lower compared with the metal component. With the plastic component develops, the structure analysis of the plastic component become get attentions. And the correlation studies on the plastic component become more and more.

However, the plastic materials contain many types, such as PP, PVC, ABS, PA and so on. These plastic materials have the low elasticity modulus and the poor structure strength. To improve the structure characteristic of the plastic materials, the engineering plastics are developed. Currently, the engineering plastics are reinforced with the carbon fiber, the glass fiber and other fibers. In addition, they are divided into two types: the short fiber reinforced plastic and the long fiber reinforced plastic. Currently, the plastic components are treated as the isotropic material for most researchers. However, the fiber has important influence on the material property. Therefore, the fiber orientation is almost impossible to ignore. For the common plastic component and the short fiber reinforced plastic, they can be treated as the isotropic material. However, for the long fiber reinforced plastic components, they should be treated as the an isotropic material.

The orientation and the number of the fibers in the plastic has important influence on the structure characteristic of the fiber reinforced plastic components. The geometry of the component and the injection process parameters such as the injection position, the number and timing of the injection pressure, the injection gates, the injection time, the mold temperature and the melt temperature can all influence the fiber distribution of the plastic component[4-7]. The elasticity modulus along the fiber orientation is large and the one normal to the fiber orientation is small. The difference makes that the long fiber reinforced components have obviously anisotropic mechanical property. Therefore, two simulations are conducted based on the isotropic material definition and the anisotropic material definition to study the difference of the thermal field, the pressure field and the vibration characteristics.

In this paper, the mold flow analysis is carried out first. The glass fiber orientation of the fiber reinforced PA66 plastic board is obtained. According to the material property parameters of the PA66 (GF 30%), the flexibility matrix of the anisotropic material is constructed. Combined the fiber orientation and the flexibility matrix, the anisotropic material definition is carried out. Next, the finite element model is constructed and the deformations and the stresses under pressure field and thermal field are calculated. Then the vibration characteristics of the two square plates with different material definitions are compared. Through the comparisons of the deformations, the stresses and the vibration characteristics, the difference and the cause are elaborated. It offers the guidance for the design and analysis of the plastic component. Elastic constitutive model of the orthogonal anisotropic material

2 Elastic constitutive model of the anisotropic material

An orthotropic material has three mutually perpendicular plates of symmetry at every point, with the intersections of these plates known as the principal axes of anisotropy [8]. Its material properties are, in general, different along different principal axis. The stress component and the strain component are not coupled. The stress-strain relationship can be defined based on the generalized Hook's law [9].

$$\{\varepsilon\}_m = [C]_m \{\sigma\}_m \tag{1}$$

$$\{\sigma\}_m = [C]_m^{-1} \{\varepsilon\}_m = [D]_m \{\varepsilon\}_m \tag{2}$$

$$\{\varepsilon\}_m = [\varepsilon_{11}\ \varepsilon_{22}\ \varepsilon_{33}\ \gamma_{12}\ \gamma_{23}\ \gamma_{31}]^T \tag{3}$$

$$\{\sigma\}_m = [\sigma_{11}\ \sigma_{22}\ \sigma_{33}\ \tau_{12}\ \tau_{23}\ \tau_{31}]^T \tag{4}$$

$$[D]_m = [C]_m^{-1} \tag{5}$$

Where ε is the strain and σ is the stress; ε_{ii} is the tensile strain and γ_{ij} the shear strain; σ_{ii} is the tensile stress and τ_{ij} is the shear stress; $[D]_m$ is the stiffness matrix and $[C]_m$ is the flexibility matrix.

$$[C]_m = \begin{bmatrix} \frac{1}{E_1} & -\frac{\mu_{21}}{E_2} & -\frac{\mu_{31}}{E_3} & 0 & 0 & 0 \\ -\frac{\mu_{12}}{E_1} & \frac{1}{E_2} & -\frac{\mu_{32}}{E_3} & 0 & 0 & 0 \\ -\frac{\mu_{13}}{E_1} & -\frac{\mu_{23}}{E_2} & \frac{1}{E_3} & 0 & 0 & 0 \\ 0 & 0 & 0 & \frac{1}{G_{23}} & 0 & 0 \\ 0 & 0 & 0 & 0 & \frac{1}{G_{13}} & 0 \\ 0 & 0 & 0 & 0 & 0 & \frac{1}{G_{12}} \end{bmatrix} \tag{6}$$

Where E_i is the tensile elastic modulus and G_{ij} is the shear elastic modulus; μ_{ij} is the poisson ratio. As the elastic matrix of orthotropic material is symmetrical, $E_1\mu_{21} = E_2\mu_{12}$, $E_2\mu_{32} = E_3\mu_{23}$ and $E_3\mu_{13} = E_1\mu_{31}$. Therefore, only 9 constants in equation (6) are independent. The constants of $[D]_m$ can be obtained through finding the inverse matrix of $[C]_m$. The stiffness matrix constants can be represented as equation (7) with the constants in equation (6).

$$\left.\begin{aligned} d_{11} &= \frac{1-\mu_{23}\mu_{32}}{E_2E_3\Delta} \\ d_{22} &= \frac{1-\mu_{13}\mu_{31}}{E_1E_3\Delta} \\ d_{33} &= \frac{1-\mu_{12}\mu_{21}}{E_1E_2\Delta} \\ d_{12} &= d_{21} = \frac{\mu_{21}+\mu_{31}\mu_{23}}{E_2E_3\Delta} = \frac{\mu_{12}+\mu_{13}\mu_{32}}{E_1E_3\Delta} \\ d_{23} &= d_{32} = \frac{\mu_{32}+\mu_{12}\mu_{31}}{E_1E_3\Delta} = \frac{\mu_{23}+\mu_{21}\mu_{13}}{E_1E_2\Delta} \\ d_{31} &= d_{13} = \frac{\mu_{13}+\mu_{12}\mu_{23}}{E_1E_2\Delta} = \frac{\mu_{31}+\mu_{21}\mu_{32}}{E_2E_3\Delta} \\ d_{44} &= G_{12} \\ d_{55} &= G_{23} \\ d_{66} &= G_{31} \end{aligned}\right\} \tag{7}$$

Where $\Delta = \dfrac{1-\mu_{12}\mu_{21}-\mu_{23}\mu_{32}-\mu_{31}\mu_{13}-2\mu_{12}\mu_{23}\mu_{31}}{E_1E_2E_3}$.

A transversely isotropic material is one with physical properties which are symmetric about an axis that is normal to a plate of isotropy [10]. This transverse plate has infinite plates of symmetry. Thus, the material properties are the same in all directions within this plate. For example, the unidirectional composite material is transversely isotropic. In a unidirectional composite, the plate normal to the fiber direction can be considered as the isotropic plan. Here the fibers would be aligned with the x1 axis, which is normal to the plate of isotropy. So the x2 axis and the x3 axis are on the plate of isotropy. Equation (8) can be obtained. Therefore the number of independent constants in the elasticity matrix is reduced to 5.

$$\left.\begin{aligned} &E_2 = E_3 \\ &\mu_{12} = \mu_{13}, \mu_{21} = \mu_{31}, \mu_{32} = \mu_{23} \\ &G_{13} = G_{12} \end{aligned}\right\} \tag{8}$$

The flexibility matrix of the transversely isotropic material can be represented as equation (9).

$$[C]_m = \begin{bmatrix} \frac{1}{E_1} & -\frac{\mu_{12}}{E_1} & -\frac{\mu_{12}}{E_1} & 0 & 0 & 0 \\ -\frac{\mu_{12}}{E_1} & \frac{1}{E_2} & -\frac{\mu_{23}}{E_2} & 0 & 0 & 0 \\ -\frac{\mu_{12}}{E_1} & -\frac{\mu_{23}}{E_2} & \frac{1}{E_2} & 0 & 0 & 0 \\ 0 & 0 & 0 & \frac{1}{G_{23}} & 0 & 0 \\ 0 & 0 & 0 & 0 & \frac{1}{G_{12}} & 0 \\ 0 & 0 & 0 & 0 & 0 & \frac{1}{G_{12}} \end{bmatrix} \tag{9}$$

Where $G_{23} = \dfrac{E_{22}}{2(1+\mu_{23})}$. The constants of stiffness matrix $[D]_m$ can be obtained through finding the inverse matrix of the flexibility matrix $[C]_m$.

3 Performance comparison of the orthogonal anisotropic material and the isotropic material

3.1 Model

To compare the mechanical properties of the orthogonal anisotropic material and the isotropic material, a square plate model of the unidirectional composite material is constructed (500×500×5 mm), shown in Figure 1. The material used is a type of PA66 with 30% fiber glass supplied by Lanxess Chemical Co. Ltd. The properties of the PA66 (GF 30%) are listed in Table 1.The location of the injection mold gate is in the middle, which makes the fiber orientation uniform.

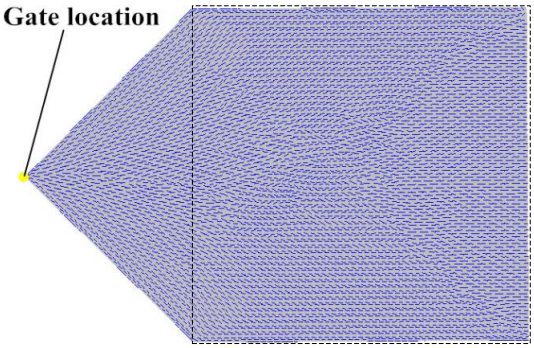

Figure 1. Model of the transversely isotropic material

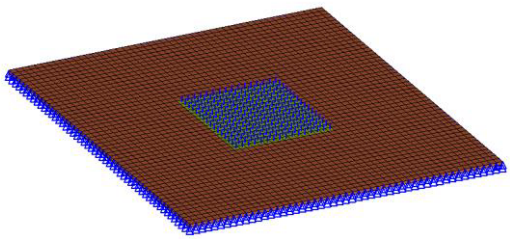

Figure 2. Boundary conditions of the square plate model

Table 1. Properties of PA66 (GF 30%).

Properties	Values
Material structure	Crystalline
Glass Fiber	30%
Solid density (g/cm^3)	1.36
Melt density (g/cm^3)	1.16
E_1 (MPa)	10300
E_2 E_3 (MPa)	6800
μ_{12} μ_{23}	0.4
G_{12} (MPa)	1910
α_1 (1/K)	3E-5
α_2 α_3 (1/K)	9E-5
Ejection temperature (℃)	185
Recommended mold temperature (℃)	90
Recommended melt temperature (℃)	300

3.2 Definition of different materials

To compare the deformations and stresses of the two materials under the same pressure, a finite element model is constructed here, shown as Figure 2. The six degrees of freedoms (DOFs) of the plate border are constrained. The square in the center of the plate is the zone of pressure. The magnitude of pressure is 0.1 MPa.

Through defining the different material properties for the finite element model, the deformations and stresses of the two plates under the same pressure are computed. The results of deformation and stress are shown in Figure 3 and Figure 4 respectively. Seen from Figure 3, the deformations of the two models are similar. It is because the four sides of the plate are all constrained. However the normal elastic modulus of the transversely isotropic material is 6800 MPa, which is smaller than the elastic modulus of the isotropic material. Therefore under the same pressure, the deformation magnitude of the transversely isotropic material plate is larger. Comparing the stresses of the two plates in Figure 4, it can be seen that the stress distribution of the isotropic material plate is central symmetrical and that of the other plate has the obvious anisotropic characteristic. As the principal elastic modulus is larger than the normal modulus, the stress along the principal direction(X axis) is larger than that along the vertical direction.

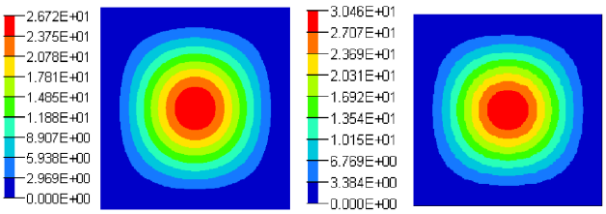

(a) Isotropic material (b) Transversely isotropic material

Figure 3. Deformation under pressure of 0.1 MPa

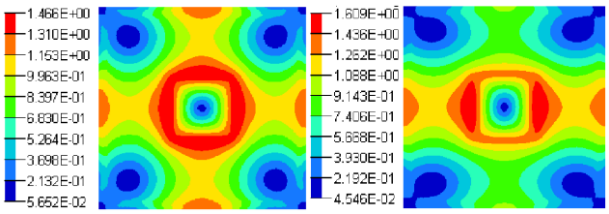

(a) Isotropic material (b) Transversely isotropic material

Figure 4. Stress under pressure of 0.1 MPa

To analyze effects of temperatures on the two materials, the boundary conditions of the square plate model are changed. The constraints are the same with Figure 2. The zone of pressure is changed to zone of T_1 and $T_1 = 323\text{K}$. The temperature of other area is set to T_2 and $T_2 = 293\text{K}$. The results of deformation and thermal stress are shown in Figure 5 and Figure 6 respectively. Seen from Figure 5 and Figure 6, the thermal deformation and stress of the transversely isotropic material plate both have the obvious anisotropic characteristic compared with the isotropic material plate. As the thermal expansion coefficient along the Y axis is larger than both that along X axis and the thermal expansion coefficient of the isotropic material,

the deformation along the Y axis is larger. As the center zone has the little temperature difference, the deformation of the zone is smaller. The Figure 6 shows that maximal thermal stress of the transversely isotropic material plate is smaller than that of the isotropic material plate in the center zone. It is because the elastic modulus along the Y axis is smaller. As the thermal deformation along the Y axis is larger, the stress is larger than that of the isotropic material plate along Y axis except the center zone. In the same way that the thermal stress along X axis is smaller.

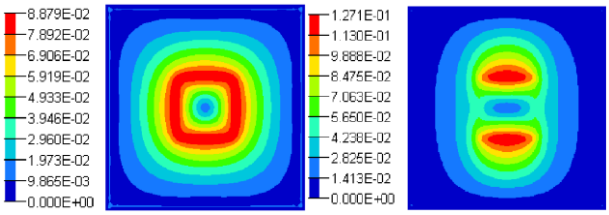

(a) Isotropic material (b) Transversely isotropic material

Figure 5. Deformation under the temperature difference of 30K

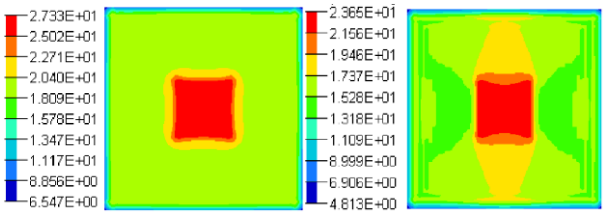

(a) Isotropic material (b) Transversely isotropic material

Figure 6. Thermal stress under the temperature difference of 30K

To compare vibration characteristics of the two square plates, the free modes are analyzed. The modal frequencies of two square plates are listed in Table 2. And the first three modal shapes are shown in Figure 7. Table 2 shows the modal frequencies of the anisotropic plate are lower than those of the isotropic plate. As the densities of the two plates are the same, it means the global stiffness of the anisotropic plate is lower than that of the isotropic plate. Figure 7 shows the first three modal shapes of the isotropic plate are all central symmetrical and the anisotropic plate is different. The first modal shape of the anisotropic plate is the first torsion and the symmetry axis is along the diagonal line (45°). As the comprehensive effects of both the principal elastic modulus and the vertical modulus, the modal shape is similar with that of the isotropic plate. However, the principal elastic modulus is larger than the vertical modulus. Therefore the second modal shape is the bending vibration along the vertical direction(Y axis) and the third modal shape is the bending vibration along the principal direction(X axis).

Table 2. Comparisons of the plate modal frequencies

Order	Isotropic	Anisotropic
1	31.29Hz	24.90Hz
2	45.92Hz	44.26Hz
3	60.59Hz	60.51Hz
4	81.93Hz	68.53Hz
5	81.93Hz	75.79Hz

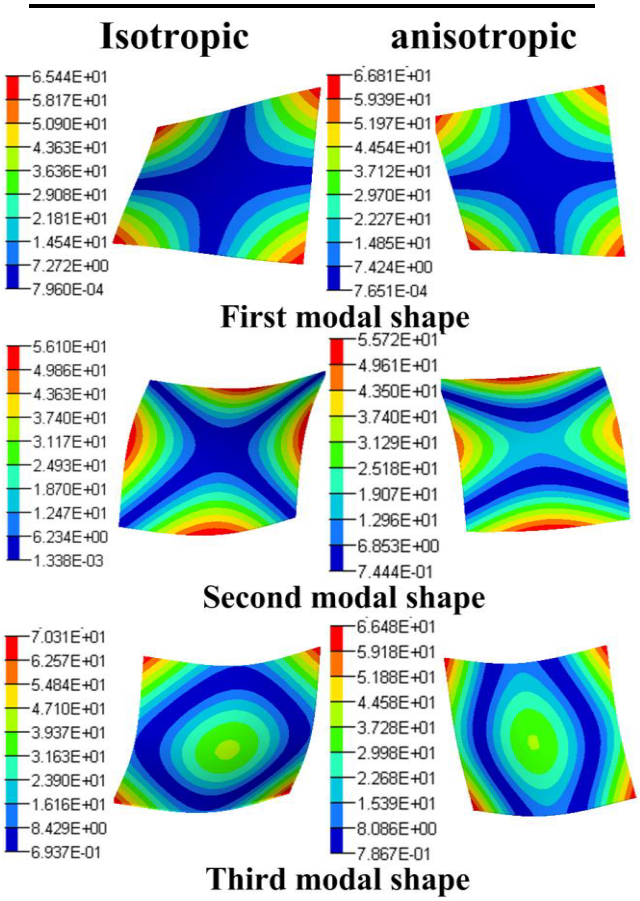

Figure 7. Comparisons of the plate modal shapes

4. Conclusions

In this study, a comprehensive performance research based on the orthotropic material was proposed. The effect of the orthotropic glass fiber reinforced PA66 characteristic on the structure performance was analyzed through the simulation of the plates with two different materials. Main conclusions can be drawn as follows:

(1)Under the same pressure, the deformation and the stress values of the transversely isotropic material plate is larger. The stress along the principal direction(X axis) is larger than that along the vertical direction.

(2)Under the same thermal boundary condition, the maximal thermal stress of the transversely isotropic material plate is smaller than that of the isotropic material plate, and the thermal deformation is larger along the vertical direction.

(3)The modal frequencies of the anisotropic plate are lower than those of the isotropic plate. The modal shapes of the transversely isotropic material plate show obvious anisotropic characteristic.

References

1. Launay A, Maitournam M H, Marco Y, et al. Cyclic behaviour of short glass fibre reinforced polyamide: Experimental study and constitutive equations[J].

International Journal of Plasticity, 2011, 27(8): 1267-1293.
2. Ku H, Wang H, Pattarachaiyakoop N, et al. A review on the tensile properties of natural fiber reinforced polymer composites[J]. Composites Part B: Engineering, 2011, 42(4): 856-873.
3. AlMaadeed M A, Kahraman R, Khanam P N, et al. Date palm wood flour/glass fibre reinforced hybrid composites of recycled polypropylene: Mechanical and thermal properties[J]. Materials & Design, 2012, 42: 289-294.
4. Gupta M, Wang K K. Fiber orientation and mechanical properties of short‐fiber‐reinforced injection‐molded composites: Simulated and experimental results[J]. Polymer Composites, 1993, 14(5): 367-382.
5. Chung S T, Kwon T H. Numerical simulation of fiber orientation in injection molding of short‐fiber‐reinforced thermoplastics[J]. Polymer Engineering & Science, 1995, 35(7): 604-618.
6. Han K H, Im Y T. Numerical simulation of three-dimensional fiber orientation in short-fiber-reinforced injection-molded parts[J]. Journal of materials processing technology, 2002, 124(3): 366-371.
7. Zhang J, Wang J, Lin J, et al. Multiobjective optimization of injection molding process parameters based on Opt LHD, EBFNN, and MOPSO[J]. The International Journal of Advanced Manufacturing Technology, 2015: 1-16.
8. Deshpande V S, Fleck N A, Ashby M F. Effective properties of the octet-truss lattice material[J]. Journal of the Mechanics and Physics of Solids, 2001, 49(8): 1747-1769.
9. Muskhelishvili N I. Some basic problems of the mathematical theory of elasticity[M]. Springer Science & Business Media, 2013.
10. Aboudi J. Mechanics of composite materials: a unified micromechanical approach[M]. Elsevier, 2013.